Progress In Electromagnetics Research C, Vol. 55, 115–127, 2014

An Approach for Efficient Two-Stage 2D-DOA Estimation in High-Altitude Platforms Mobile Communications

Yasser Albagory[1, 2, *]

Abstract—High-Altitude Platform (HAP) is a promising technique for providing wireless communications services with improved performance compared to terrestrial and satellite systems. A critical issue in this emerging system is the difficulty of providing user location information through two-dimensional direction-of-arrival (2D-DOA) estimation due to the high computational complexity and the large covered area. Therefore, in this paper, an efficient technique has been proposed to determine user location through 2D-DOA with a reduced processing time. The proposed technique estimates the 2D-DOA in two stages. In the first stage, a low-resolution 2D-DOA estimation technique will be utilized, such as Bartlett algorithm performed on a low-resolution distance grid, then a suitable threshold is applied on the normalized Bartlett 2D-DOA spectrum to define ground windows for the next high-resolution 2D-DOA stage. The second stage is carried out by a high-resolution technique such as MUSIC algorithm and will be performed on a high-resolution distance grid. Two scenarios are examined for the proposed technique to investigate the reduction in processing time compared with the conventional 2D-DOA MUSIC algorithm without windowing. Simulation results show that at 40 meters resolution, the required processing time is only 20% of the conventional MUSIC algorithm and can be further reduced to 4% at resolution of 100 meters at the same array size. In addition, the proposed technique can be applied to any other efficient low-complexity 2D-DOA algorithms.

1. INTRODUCTION

Recently, there is increasing interest in developing high-altitude platforms (HAP) for wireless communications due to their advantages compared to the conventional terrestrial and satellite systems [1–4]. HAP are airships or aircrafts flying in the stratosphere at altitudes ranging from 20 to 50 km with a preferable height of 20 km at which the wind speed is almost minimum [5]. HAP can provide superior performance for different communication services including mobile communications, broadcasting, remote sensing and military applications. In addition, HAP communication system can be used as a complement to terrestrial and satellite systems due to its economical benefits and flexibility in the infrastructure. Many of the HAP communications applications depend on the user location which explores a set of *location-dependent services*. Localization of users may be established by Global Positioning System (GPS) [6] where each mobile handset should have a GPS receiver and must exist in an open sky area to get his location information accurately. The location applications require feedback and agreement from users to access their GPS information or to use their location information obtained from the ground communications network. At critical and emergency times, the system should have accurate location information about users where another complement technique has to be used especially for mobile phones that have no GPS capability or because the users in this case are almost not able to provide their location information by themselves or even communicate to acquire a rescue. Another

Received 24 October 2014, Accepted 2 December 2014, Scheduled 11 December 2014

* Corresponding author: Yasser Albagory (y.a.albagory@ieee.org).

[1] Department of Electronics and Electrical Communications Engineering, Faculty of Electronic Engineering, Menoufia University, Egypt. [2] College of Computers and Information Technology, Taif University, KSA.

technique for determining user location is to develop direction-of-arrival (DOA) estimation technique independently on the GPS system. In HAP systems, DOA estimation techniques should provide two-dimensional angles-of-arrival for users with high accuracy as well as reduced computation complexity for fast detection. The coverage area of a single HAP may be several hundreds of square kilometers, which necessitates the use of a large size antenna array and consequently is very extensive and has huge processing burden for estimating DOAs especially when applying high resolution techniques such as MUltiSIgnal Classification (MUSIC) algorithm [7]. Several studies [8–13] have proposed and developed techniques for reducing the processing time for the two-dimensional (2D)-DOA estimation including the modification in the algorithms or the array configuration.

The 2D-DOA estimation for HAP unfortunately not only requires large array size to detect larger number of signals, but also needs to search the covered area with high-resolution distance grid, which adds another complexity in the system. Therefore in this paper, the main objective is to develop a 2D-DOA estimation technique that supports high-resolution estimation techniques with a reduced total processing time for accurate and fast user location determination. This proposed technique starts with pre-scanning the HAP coverage area with low-complexity low-resolution technique such as Bartlett algorithm [14], and then filters out the areas apart from the peaks in the Bartlett normalized spectrum and considering only the portion around the expected DOA peaks for subsequent high-resolution MUSIC 2D-DOA stage. The filtering operation will be accomplished by applying a suitable threshold on the Bartlett normalized spectrum which subsequently reduces the total processing time greatly according to the DOAs distribution.

The paper is organized as follows. Section 2 provides a geometrical description about HAP system and a search grid for the 2D-DOA algorithms, while Section 3 describes the array geometry and signal model required for DOA estimation. In Section 4, the proposed algorithm is demonstrated, and Section 5 provides the simulation results for two case studies for the sources distribution. Finally, Section 6 concludes the paper.

2. HAPS SYSTEM GEOMETRY FOR DOA ESTIMATION

Defining the HAP system geometry for 2D-DOA estimation is very important as it defines the relation between the HAP position and user's location as well as the search points and directions for the different algorithms.

2.1. DOA Grid Co-Ordinate System for HAP

An antenna array on HAP will have inverted Cartesian co-ordinates as shown in Figure 1, where the array power spectrum is directed downward. The coverage area per HAP is assumed to be a square of

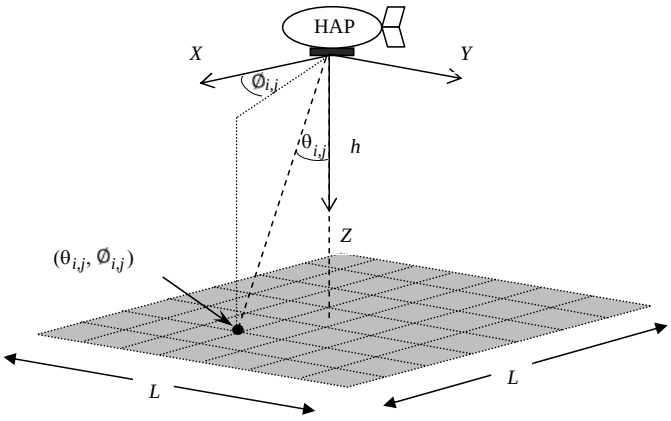

Figure 1. HAP co-ordinate system and ground search grid for 2D-DOA estimation.

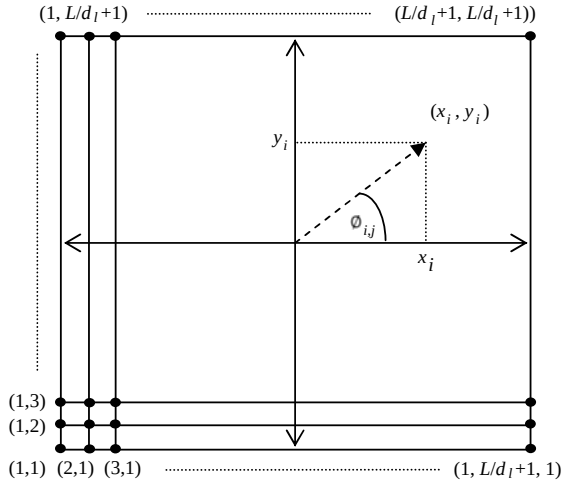

Figure 2. Ground search grid for 2D-DOA estimation.

$L \times L$ km, and this area is further subdivided into a grid of points that will be used as search points for the 2D-DOA algorithms.

An initial low-resolution distance between grid points d_l is used in the low-complexity low-resolution 2D-DOA estimation stage. In the subsequent high-resolution stage, another high-resolution distance and condensed grid points with distance separation of d_h are applied. It is clear that the value of d_h is much smaller than d_l to gain high-resolution and accurate 2D-DOA angles. The HAP height is h, and its sub-HAP point is located at the center of the coverage.

The ground search matrix containing points (i, j) defines the locations at which the algorithm estimates the DOA spectrum. This matrix is also denoted as ground search grid and depicted in Figure 2, where at each grid point (i, j), there is a corresponding angle direction $(\theta_{i,j}, \emptyset_{i,j})$ which can be related to the system geometry by the following equations:

$$\theta_{i,j} = \tan^{-1}\left(\frac{d(i,j)}{h}\right) \tag{1}$$

$$\emptyset_{i,j} = \tan^{-1}\left(\frac{y_j}{x_i}\right) \tag{2}$$

where

$$d(i,j) = \sqrt{x_i^2 + y_j^2} \tag{3}$$

and

$$x_i = (i-1)\, d_l - \frac{L}{2} \tag{4}$$

$$y_j = (j-1)\, d_l - \frac{L}{2} \tag{5}$$

where x_i and y_j are the ground co-ordinates of the search point (i, j).

The distance d_l in (4) and (5) is replaced with d_h when we use the high-resolution 2D-DOA algorithm. It also defines the accuracy of finding the user location as the ground grid points are separated by multiple of d_h in either directions of X and Y.

2.2. Expanding Ground Search Grid for High Resolution Distances

In this section, we will describe the expansion process from a low-resolution grid into a high-resolution grid in the same area. Figure 1 depicts the system geometry where the HAP is located at an altitude

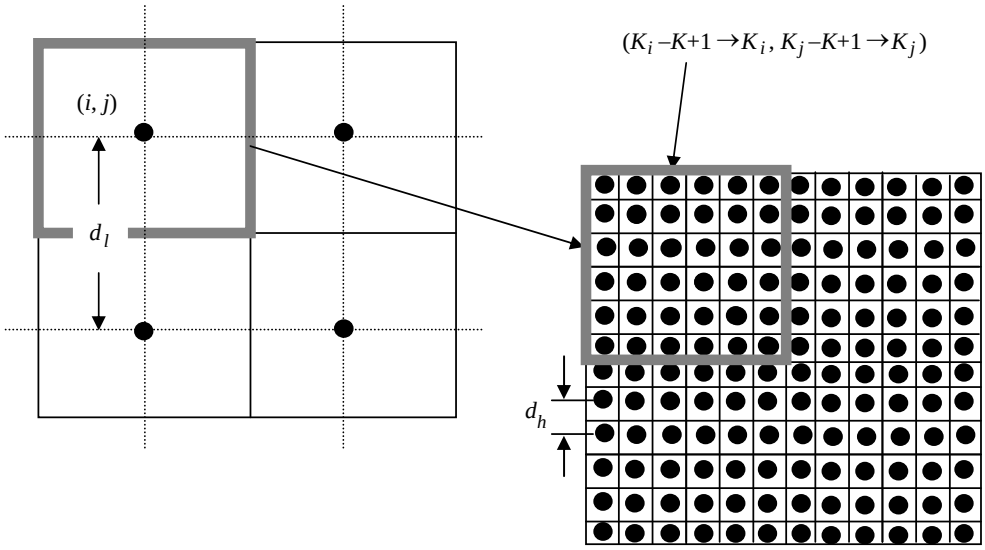

Figure 3. Ground search grid expansion for high-resolution 2D-DOA estimation stage.

h and covers a square area of dimensions $L \times L$ km in the two directions. This area is divided into a grid of points separated initially by a large inter-point distance d_l and will be used in the first stage, then after threshold stage, smaller patches of this grid are expanded into higher number of grid points of separation d_h in the same area.

If the number of points in the smaller grid area is expanded by a factor K, then the grid expansion process can be obtained replacing a point (i, j) by a new grid given by:

$$(i, j) \rightarrow (K_i - K + 1 : K_i, K_j - K + 1 : K_j) \tag{6}$$

According to the grid expansion, the search angles will map as follows:

$$(\theta_{i,j}, \emptyset_{i,j}) \Rightarrow \begin{pmatrix} \left(\theta_{K_i-K+1,K_j-K+1}, \emptyset_{K_i-K+1,K_j-K+1}\right) & \cdots & \left(\theta_{K_i-K+1,K_j}, \emptyset_{K_i-K+1,K_j}\right) \\ \vdots & \ddots & \vdots \\ \left(\theta_{K_i,K_j-K+1}, \emptyset_{K_i,K_j-K+1}\right) & \cdots & \left(\theta_{K_i,K_j}, \emptyset_{K_i,K_j}\right) \end{pmatrix} \tag{7}$$

The new grid points after expansion is shown in Figure 3.

3. SIGNAL MODEL

In array processing, each antenna element in an array is usually considered as an isotropic radiator or sensor, and the different impinging signals form plane wavefronts where the delay between successive elements is the same in uniform linear array structures. For any DOA algorithm, the signal model should be defined to determine the array covariance matrix. In this paper, we will utilize uniform circular array which is a popular configuration for DOA estimation and can provide 2D-DOA. Other array geometries may also be applied such as L-shaped array [15]. The number of antenna elements is assumed to be M and uniformly interspaced with half of wavelength distance. Assuming D narrowband signals impinging on the array with different directions, the signals data at the array elements can be described by $(M \times 1)$ vector given by:

$$\mathbf{x}(t) = \mathbf{A}(\theta, \emptyset)\, s(t) + \mathbf{n}(t) \tag{8}$$

where $\mathbf{A}(\theta, \emptyset) = [\mathbf{a}(\theta_1, \emptyset_1), \mathbf{a}(\theta_2, \emptyset_2), \ldots, \mathbf{a}(\theta_D, \emptyset_D)]$ is the array manifold which contains information on DOAs of the incident signals, and $\mathbf{n}(t)$ is the additive noise vector at the array sensors.

For the circular arrays, with half-wavelength interelement spacing $\mathbf{a}(\theta_i, \emptyset_i)$ is given by:

$$\mathbf{a}(\theta, \emptyset) = \left[e^{j\frac{M}{2}\sin(\theta)\cos\left(\emptyset - \frac{2\pi}{M}\right)} \quad e^{j\frac{M}{2}\sin(\theta)\cos\left(\emptyset - \frac{4\pi}{M}\right)} \quad \cdots \quad e^{j\frac{M}{2}\sin(\theta)\cos(\emptyset - 2\pi)} \right]^T \tag{9}$$

After weighting the received signals by $\mathbf{W}$, the output is given by:

$$\mathbf{y}(t) = \mathbf{W}^H \mathbf{x}(t) \tag{10}$$

where $\mathbf{W}^H$ is the Hermitian or complex conjugate transpose of the array weighting vector.

The output $\mathbf{y}(t)$ can be rewritten as:

$$\mathbf{y}(t) = \mathbf{W}^H \mathbf{A}(\theta, \emptyset)\, s(t) + \mathbf{W}^H \mathbf{n}(t) \tag{11}$$

where $\mathbf{W}^H \mathbf{n}(t)$ is the additive noise at the beamformer output.

Assuming that the incident signals are uncorrelated and independent of the noise at the antenna elements, under this condition and assuming equal noise powers at the different array elements, the array input covariance matrix is given by:

$$\mathbf{R}_{xx} = \mathbf{A}(\theta, \emptyset)\, E\left[\mathbf{s}(t)\, \mathbf{s}^{\mathbf{H}}(t)\right] \mathbf{A}^{\mathbf{H}}(\theta, \emptyset) + E\left[\mathbf{n}(t)\, \mathbf{n}^{\mathbf{H}}(t)\right] = \mathbf{A}(\theta, \emptyset)\, \mathbf{R}_{ss} \mathbf{A}^{\mathbf{H}}(\theta, \emptyset) + \sigma^2 \mathbf{I} \tag{12}$$

where $\mathbf{R}_{ss} = E[\mathbf{s}(t)\mathbf{s}^{\mathbf{H}}(t)]$ is the sources covariance matrix, σ^2 the noise power at the array elements, and $\mathbf{I}$ the identity matrix (with dimensions $M \times M$).

3.1. Bartlett Beamformer for 2D-DOA

In this method, the array collects the signals such that the output of the beamformer is maximized at the signal directions. The array output power at a certain weight vector $\mathbf{W}(\theta, \emptyset)$ is given by:

$$P_B(\theta, \emptyset) = \frac{1}{N} \sum_{n=1}^{N} |y(t)|^2 \tag{13}$$

or

$$P_B(\theta, \emptyset) = \frac{1}{N} \sum_{n=1}^{N} \mathbf{W}^H(\theta, \emptyset)\, \mathbf{x}(t)\, \mathbf{x}^H(t)\, \mathbf{W}(\theta, \emptyset) \tag{14}$$

and

$$\widehat{\mathbf{R}_{xx}} = \frac{1}{N} \sum_{n=1}^{N} \mathbf{x}(t)\, \mathbf{x}^H(t) \tag{15}$$

where N is the number of samples and $\widehat{\mathbf{R}_{xx}}$ the maximum likelihood estimation of $\mathbf{R}_{xx}$.

The power maximization process at the signal direction depends on the chosen array weight vector, and in Bartlett beamformer it has been chosen as the array steering matrix $\mathbf{a}(\theta, \emptyset)$. Therefore, the Bartlett angular power spectrum will be:

$$P_B(\theta, \emptyset) = \mathbf{a}^H(\theta, \emptyset)\, \widehat{\mathbf{R}_{xx}} \mathbf{a}(\theta, \emptyset) \tag{16}$$

The DOAs are checked at the peaks of $P_B(\theta, \emptyset)$. If the sources are very near or at least separated by less than the array beamwidth, this beamformer cannot resolve these signals and will be collected under one 'wider' peak.

The Bartlett DOA estimation will be just a guide to reduce the search range in the high-resolution grid stage so that it will start by calculating DOAs with low-resolution grid.

3.2. MUSIC 2D-DOA Estimation

For the subspace techniques such as MUSIC algorithm, it is required to describe the array covariance matrix by its eigenvalues and eigenvectors as follows:

$$\mathbf{R}_x = \mathbf{E}_s \mathbf{\Lambda}_s \mathbf{E}_s^H + \mathbf{E}_n \mathbf{\Lambda}_n \mathbf{E}_n^H \tag{17}$$

where

$$\mathbf{E}_s \mathbf{\Lambda}_s \mathbf{E}_s^H = \sum_{i=1}^{D} \lambda_i \mathbf{e}_i \mathbf{e}_i^H \tag{18}$$

and

$$\mathbf{E}_n \mathbf{\Lambda}_n \mathbf{E}_n^H = \sigma^2 \sum_{i=D+1}^{M} \mathbf{e}_i \mathbf{e}_i^H \tag{19}$$

where the $\mathbf{E}_s = [\mathbf{e}_1, \mathbf{e}_2, \ldots, \mathbf{e}_D]$ and $\mathbf{E}_n = [\mathbf{e}_{D+1}, \mathbf{e}_{D+2}, \ldots, \mathbf{e}_M]$ are the signal and noise subspaces, respectively, and contain the eigenvectors corresponding to the signal and noise. The diagonal matrix $\mathbf{\Lambda} = \mathrm{diag}[\lambda_1, \lambda_2, \ldots, \lambda_M]$ contains the eigenvalues arranged in descending order with D highest values corresponding to the signal eigenvalues, and the remaining M-D are corresponding to the noise eigenvalues.

MUSIC technique provides high angular resolution DOA estimation. It is based on the assumption that signal vectors are perpendicular to noise subspace. Another assumption is that the sources should also be uncorrelated.

The MUSIC angular power spectrum is defined as [7]:

$$\mathbf{P_M}(\theta, \emptyset) = \frac{1}{|\mathbf{a^H}(\theta, \emptyset)\, \mathbf{E_n} \mathbf{E_n^H} \mathbf{a}(\theta, \emptyset)|} \tag{20}$$

4. THE PROPOSED ALGORITHM

The intensive calculations of MUSIC 2D-DOA can be reduced by applying windows on the search angular range after spatial filtering by a threshold over the Bartlett output power spectrum. One important notice is that according to the number of sources and the angular separation between them, the peaks in the Bartlett spectrum will be different in magnitude. Therefore, it is essential to normalize the power pattern to ease the application of the threshold.

Therefore, the high-resolution algorithm is expected to take less time to find the DOAs according to the size of the filtered search area. The higher the threshold value (i.e., near 0 dB) is, the smaller the search area is around the exact DOAs, and the lesser the processing time is. This is actually true if the sources are sparsely localized or at least separated by angles more than the array beamwidth. On the other hand, when the sources are very close and others are sparsely separated, one should reduce the threshold value to accommodate the regions of the sparsely separated or isolated sources.

Figure 4 shows the proposed algorithm block diagram which executes the following steps:

1- Define the initial low-resolution grid points that scan the coverage area of the HAP.
2- Calculate the array covariance matrix, $\widehat{\mathbf{R}_{xx}}$.
3- Calculate the Bartlett power spectrum, $P_B(\theta, \emptyset)$
4- Apply a suitable low threshold on $P_B(\theta, \emptyset)$ and determine the filtered output grid points $(\theta_{i,j}, \emptyset_{i,j})$.
5- Expand the output low-resolution grid points $(\theta_{i,j}, \emptyset_{i,j})$ to the high-resolution grid points using (7).
6- Calculate the high resolution DOAs using MUSIC algorithm over the expanded grid points.
7- If there are some very close DOAs detected, reduce the threshold value and repeat steps from 4 to 6 as there may be other dropped DOAs in the last threshold operation within the HAP area.

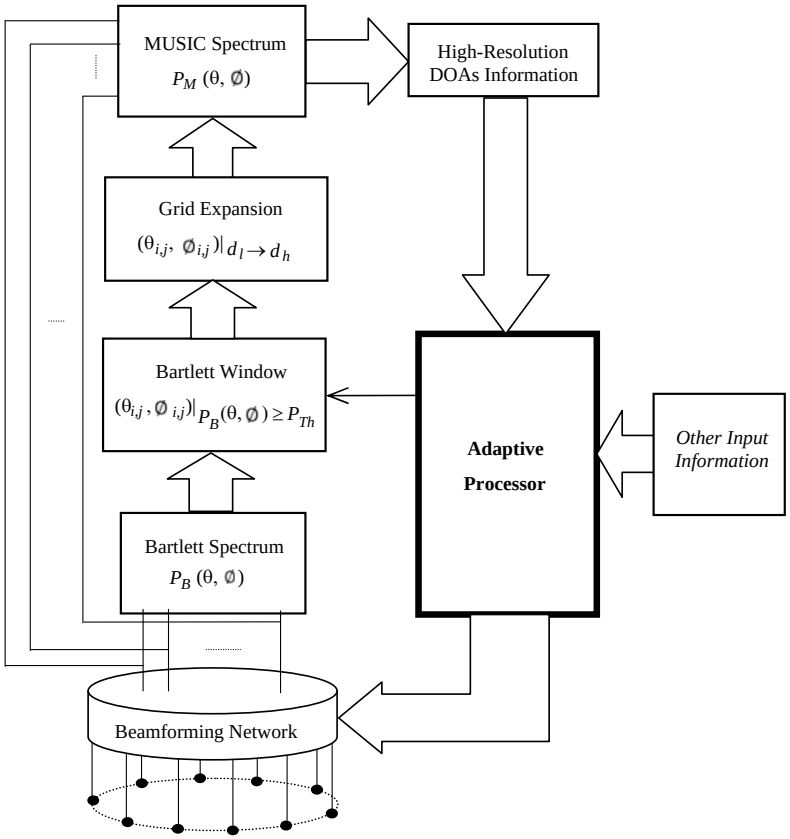

Figure 4. Block diagram of the proposed algorithm.

5. SIMULATION RESULTS

In this section, the proposed technique will be examined in two case studies. The first is for independent sources that are spaced apart, and their angular separation is greater than the array beamwidth. The second case assumes a group of close sources that lie within the array beamwidth, and the capability of the algorithm is examined to detect these sources at different threshold levels.

5.1. Case Study 1: Sources Are Spaced Apart in Place

The following parameters in Table 1 are assumed in this case study where eight isolated sources are processed for estimating their DOAs.

The area span is a square of 40 km length, and the distance resolution is 400 m initially and 40 m for high-resolution 2D-DOA estimation stage. The antenna array is a uniform circular array with half-wavelength interelement spacing. This array will provide beamwidths ranging from 13° (at direction of

Table 1. System parameters for the first case study.

Array size	20 elements
Array type	Circular Array
Interelement separation	0.5λ
Coverage Span	40 km
Low-resolution distance (d_B)	400 m
High-resolution distance (d_M)	40 m
K factor	10
Number of snapshots (N)	1024
HAP height	20 km
Range of Array Beamwidth (for delay and sum beamformer without tapering)	13° (Boresight) −17.5° (Edge-of-Coverage)
Sources Directions or DOAs	(0, 0), (20, 0), (20, 320), (40, 40), (30, 90), (20, 120), (30, 150), and (35, 200)
Signal-to-Noise Ratio (dB)	20 dB
Threshold (dB)	−2 dB

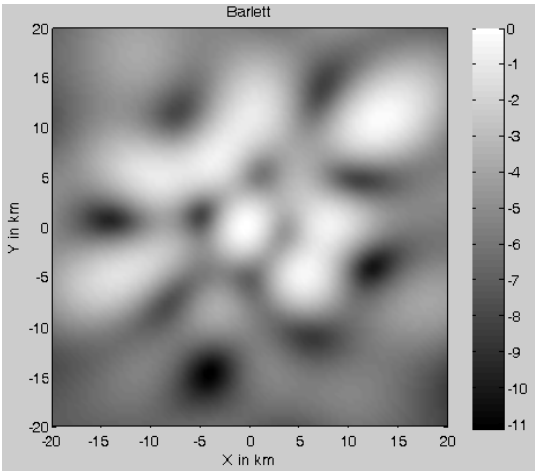

Figure 5. Normalized Bartlett DOA spectrum showing the white peaks at the sources DOAs.

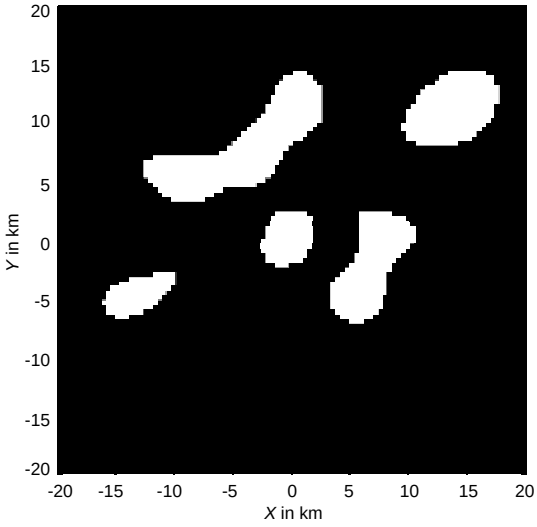

Figure 6. The area filter output for subsequent MUSIC 2D-DOA estimation.

(0°, 0°) corresponding to boresight direction or towards the sub-platform point) to 17.5° (at direction (45°, 0°) corresponding to the edge of coverage). The sources are assumed to be spaced apart and have directions as in the table. The sources directions are the actual angle directions from the HAP towards the sources using the HAP coordinates and form the real locations of those sources. The threshold is chosen −2 dB which is very close to the peaks that will appear in the Bartlett normalized spectrum. The assumption of spaced sources is advantageous in assuming high threshold value which subsequently produces small windows for searching for the high-resolution DOAs and hence reduces processing time. Figure 5 displays the Bartlett normalized spectrum (in gray-scale) where most white areas correspond to the sources DOAs.

The next step is to filter out the areas apart from these peaks by applying the threshold as shown in Figure 6.

The white areas will define where to expand the search grid matrix using (7).

The MUSIC algorithm is then applied with the high-resolution distance d_h over the white areas only. The output MUSIC 2D-DOA spectrum is shown in Figure 7 where very narrow peaks appear in the spectrum corresponding to the sources locations. The number of peaks is the same as the number of sources, so there are no missing sources in the estimation procedure after filtering the area.

A pure view for the 2D-DOAs is shown in Figure 8 where the spectrum in Figure 7 is filtered and refined at −30 dB.

A rough estimation of how the processing time will be reduced is to find the ratio of white area to whole area, but actually another process including Bartlett spectrum calculation should be added to the total processing time.

It is clear from the last two timing figures that the proposed technique has reduced the total processing time by a ratio given by:

$$T_r = \frac{T_{Rxx} + T_{\text{Bartlett}} + T_{\text{WMUSIC}}}{T_{Rxx} + T_{\text{MUSIC}}} \tag{21}$$

where:

T_r: Processing time reduction ratio,

T_{Rxx}: Calculation time for the input covariance matrix,

T_{Bartlett}: Calculation time for the Bartlett DOA spectrum,

T_{WMUSIC}: Calculation time for the windowed MUSIC,

T_{MUSIC}: Calculation time for classic MUSIC without windowing.

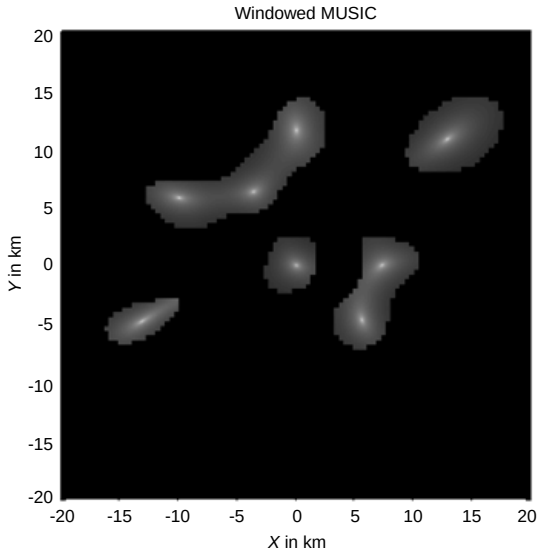

Figure 7. MUSIC 2D-DOA location spectrum.

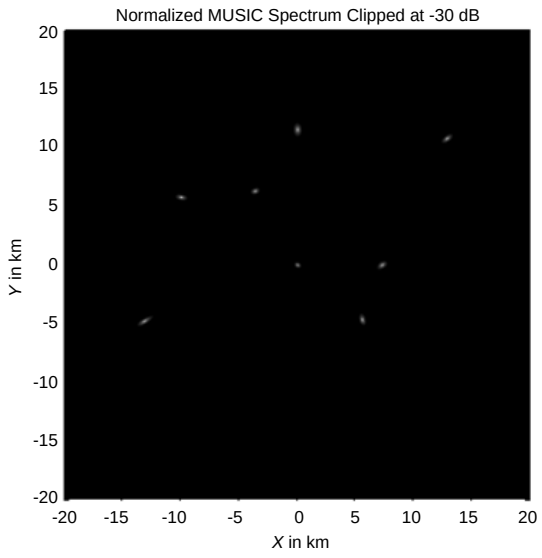

Figure 8. Refined MUSIC 2D-DOA location spectrum at −30 dB showing clearly the detected sources locations.

Figure 9 displays the processing time needed in calculating 2D-DOA spectrum for the proposed technique where it shows separately the time of calculating the covariance matrix, Bartlett spectrum, and MUSIC 2D-DOA. Other processing times such as applying the threshold and search grid expansion are very small and negligible. The Bartlett spectrum calculations take a time which is almost consumed in the covariance matrix calculations while in MUSIC there will be a matrix inversion and other matrix multiplications. In Figure 10, the regular MUSIC 2D-DOA is calculated (i.e., without Bartlett spectrum calculations and windowing) where the processing time is also split into two times corresponding to the covariance matrix calculations and MUSIC algorithm respectively.

From Figures 9 and 10, in this case study, the total processing time for calculating the proposed windowed MUSIC algorithm will be only 0.18 of the classic MUSIC processing time.

5.2. Case Study 2: Sources are Very Close in Place

In the second case study, some of the sources are brought together and will occupy an area smaller than that covered by the smallest beamwidth of the array. This will affect the Bartlett spectrum where the

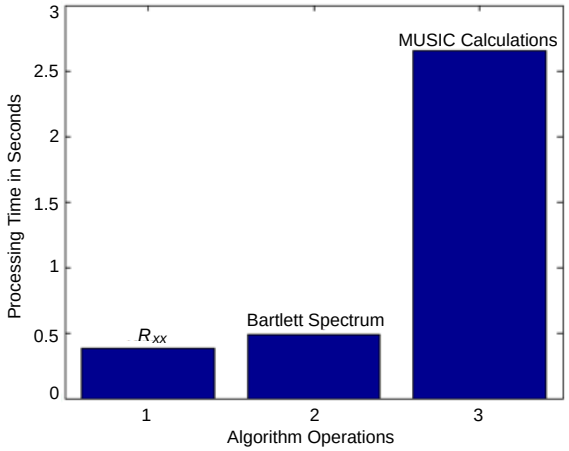

Figure 9. Processing time for the different stages in the proposed 2D-DOA technique.

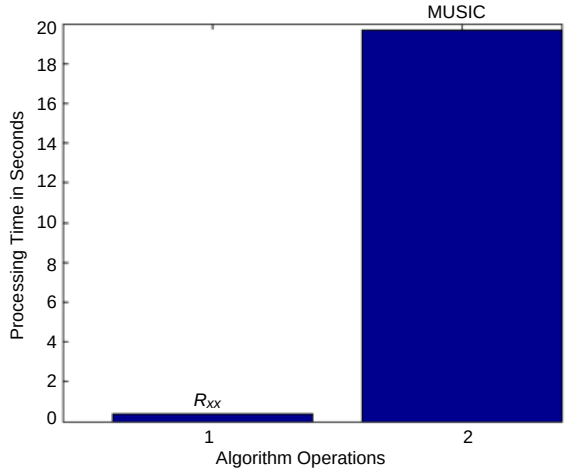

Figure 10. Processing time for the conventional MUSIC 2D-DOA technique.

Table 2. System parameters for the second case study.

Array size	20 elements
Array type	Circular Array
Interelement separation	0.5λ
Coverage Span	40 km
Low-resolution distance (d_B)	400 m
High-resolution distance (d_M)	40 m
K factor	10
Number of snapshots (N)	1024
HAP height	20 km
Range of Array Beamwidth (for delay and sum beamformer without tapering)	13° (Boresight) −17.5° (Border-of-Coverage)u
Source Directions	(0, 0), (10, 0), (10, 270), (10, 180), (30, 90), (20, 120), (30, 150), and (35, 200)
Signal-to-Noise Ratio (dB)	20 dB
Threshold (dB)	−2 dB, −3 dB

close sources produce almost one wide peak while the other far sources produce individual peaks but at lower values. This will make a constraint on choosing the threshold value because higher threshold values may cause a loss of some DOAs in the MUSIC stage.

The system parameters are shown in Table 2 where two threshold values will be checked. The sources directions or DOAs relative to HAP location and co-ordinates are modified from that in Table 1 where four of them are brought together.

The Bartlett spectrum is shown in Figure 11, where the nearby sources produce a wide white area of one peak at the center of the graph. The other remote sources provide their own peaks but at darker areas which mean that their peaks in the spectrum are lower than that corresponding to the nearby sources.

In the next step of thresholding, we will start with a lower threshold value of −3 dB. The resulted filtered area is shown in Figure 12, and the resulted windowed MUSIC 2D-DOA spectrum is shown in Figure 13 where the peaks are very close to the window edges. This means that the threshold value is

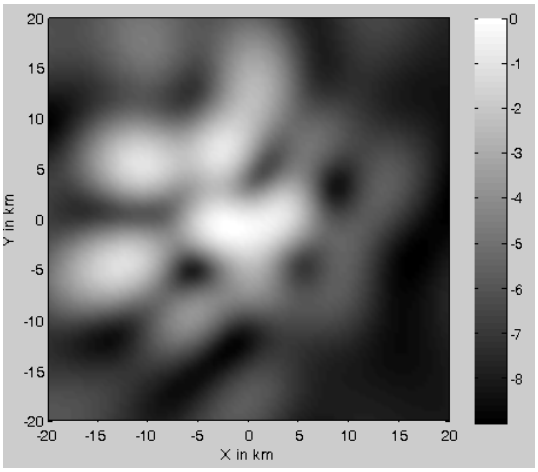

Figure 11. Bartlett 2D-DOA Spectrum for the second case study.

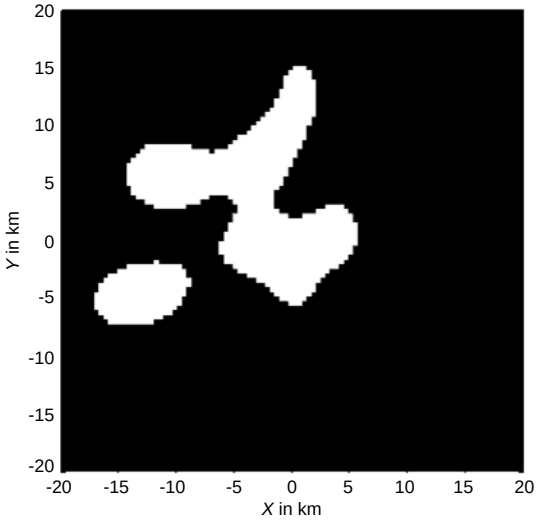

Figure 12. The area filter output at threshold value of −3 dB.

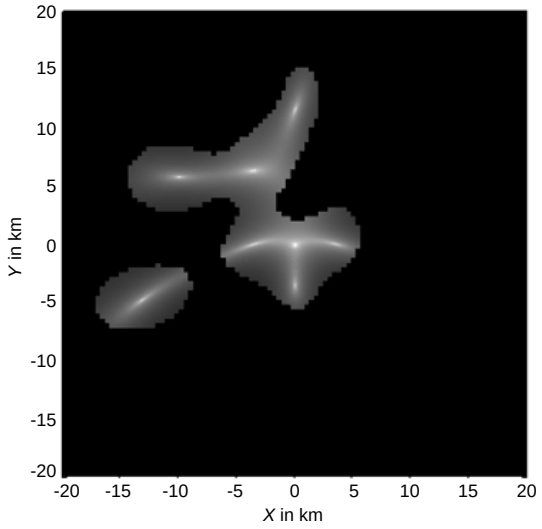

Figure 13. MUSIC 2D-DOA location spectrum at −3 dB threshold.

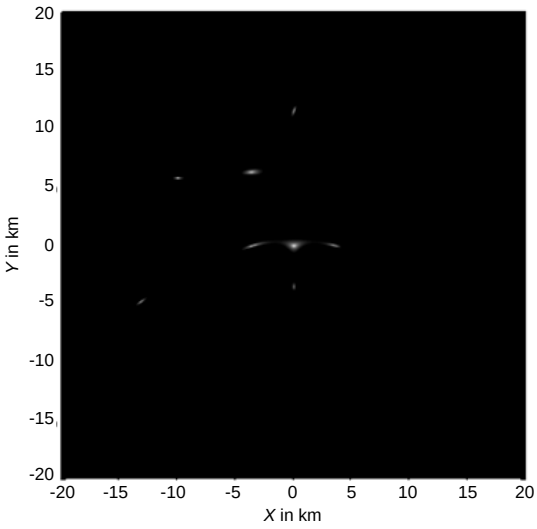

Figure 14. Smoothed MUSIC 2D-DOA location spectrum at −3 dB threshold.

critical, and any increase in the threshold value may cause a loss in the detected DOAs. The smoothed MUSIC 2D-DOA location spectrum is shown in Figure 14 where it demonstrates the capability of detecting DOAs of the sources lying inside the area of the array beamwidth which is an advantage that could not be obtained in Bartlett algorithm.

The effects of raising threshold value to −2 dB is demonstrated in Figures 15 and 16 where in the first figure the filtered area is smaller than that in Figure 12 which means higher detection speed for the DOAs, but in fact one source DOA is lost as shown in Figure 16.

Therefore, there is a compromise between the speed of calculation and the accuracy in detecting DOAs especially in the case of close spaced sources.

The processing time will mainly depend the threshold value on (at constant array size and distance resolution) where lower threshold values result in more processing time and may exceed at some values compared to the conventional MUSIC 2D-DOA algorithm. The variation of processing time (using

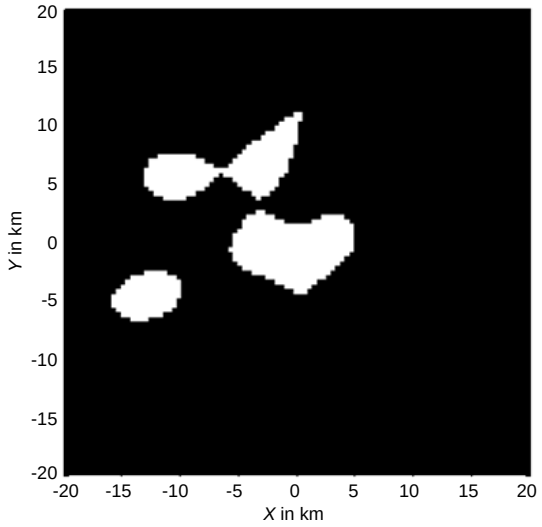

Figure 15. The area filter output at threshold value of −2 dB.

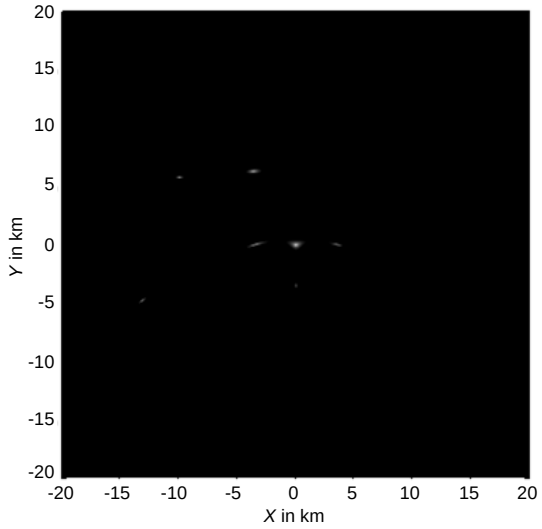

Figure 16. Smoothed MUSIC 2D-DOA location spectrum at −2 dB threshold showing 7 sources only.

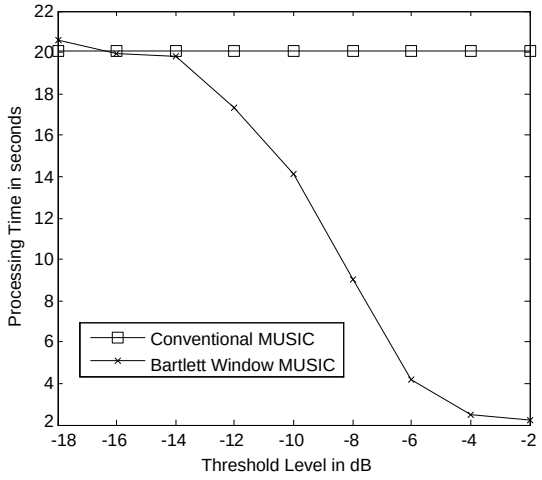

Figure 17. Processing time variation with threshold value for the windowed and conventional MUSIC algorithm.

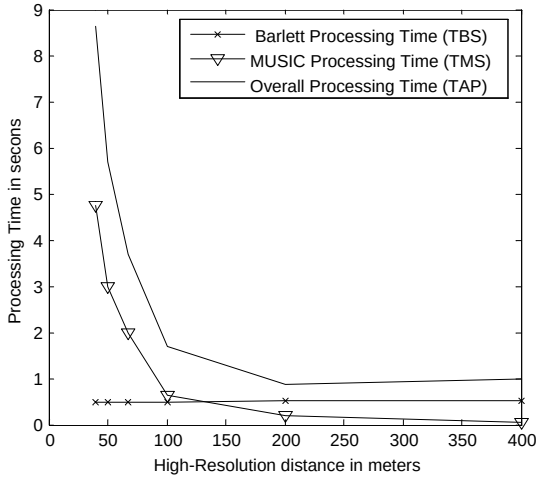

Figure 18. Processing times variation with the high-resolution distance for the proposed algorithm.

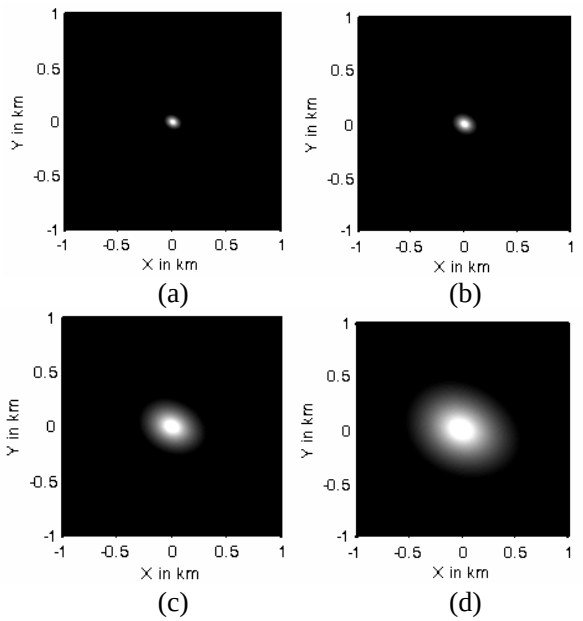

Figure 19. Effect of reduced SNR value on the accuracy of DOA estimation. SNR = 20 dB, (b) SNR = 10 dB, (c) SNR = 5 dB, and (d) SNR = 1 dB.

MATLAB, Core i3 processor, 3 MB cash and 8 GB RAM platform) with the threshold value is depicted in Figure 17 where the sensed reduction in processing time will appear at threshold values greater than −10 dB. At much lower threshold values (e.g., −18 dB), the processing time will exceed the conventional MUSIC algorithm because the window will not filter out any areas, and an extra time for the Bartlett spectrum (T_{Bartlett}) will add to the overall processing time without any benefit. At high threshold values near −3 dB, the processing time will be reduced to considerable values compared with conventional MUSIC algorithm, and the percentage of reduction will be 80% approximately at threshold value of −4 dB and by 85% at −2 dB.

On the other hand, the overall processing time will also depend on the high-resolution distance, and Figure 18 shows this variation at threshold value of −4 dB. The processing time will be reduced greatly when we increase the value of d_h from 40 m to 100 m, and the amount of reduction is 80% where TBS is the time needed for Bartlett calculations and is determined only at 100 m. TMS is the MUSIC calculation time, and TAP is the total processing time. Therefore, at 100 m resolution, the overall processing time can be reduced to only 4% of that required at 40 m resolution and without windowing which means that there is another compromise between the distance accuracy and the speed of detection.

Finally, we will check the capability of the proposed technique to detect sources at lower SNR values. We will examine the first case study at different SNR values starting with 20, 10, 5, and 1 dB, respectively. Figure 19 demonstrates this problem where the effect will be in the form of reduced location accuracy as the peaks in the DOA spectrum will have wider spots around the exact mobile station location. In this figure, we have checked the source at (0, 0) and focus on its location within a box of 2×2 km in the 2D-DOA spectrum. The peak corresponding to this source becomes wider if the SNR is reduced and the black areas correspond to values in the spectrum less than −30 dB. Therefore, the system still have the capability of detecting DOAs even at very low SNR values, but the accuracy will be worse than at higher SNR values.

6. CONCLUSION

In this paper, an algorithm for 2D-DOA estimation in the HAP mobile communications system has been proposed where the high-resolution MUSIC algorithm is performed on angular windows that

are obtained by a low-resolution Bartlett spectrum. The technique has started with low-resolution Bartlett algorithm calculated on a low resolution distance grid for sources pre-scanning, then the areas around sources are filtered by taking a suitable threshold on the Bartlett normalized spectrum, and the resulting windows are then expanded for high-resolution distance grid for the subsequent high-resolution MUSIC stage. The total processing time has been reduced by considerable values especially at higher threshold values near 0 dB. The problem of detecting closely spaced sources in the Bartlett stage has been compromised by choosing a bit lower threshold value which is necessary to avoid losing of sources at the cost of more processing time. Finally, the system is capable of detecting signals at very low SNR values at the cost of lower accuracy of location.

REFERENCES

1. Pavlidou, F. N., M. Ruggieri, M. Gerla, and R. Miura, "Communications via high altitude platforms: Technologies and trials," *International Journal of Wireless Information Networks*, Vol. 13, No. 1, 1–4, Jan. 2006.
2. Mohammed, A., S. Arnon, D. Grace, M. Mondin, and R. Muira, "Advanced communication techniques and applications for high altitude platforms," *EURASIP International Journal of Communications and Networking*, Vol. 2008, 934837, 2008.
3. Mohammed, A., A. Mehmood, F. N. Pavlidou, and M. Mohorcic, "The role of high-altitude platforms (HAPs) in the wireless global connectivity," *Proceedings of the IEEE*, Vol. 99, No. 11, 1939–1953, Nov. 2011.
4. Kim, J., D. Lee, J. Ahn, D. S. Ahn, and B. J. Ku, "Is HAPS viable for the next-generation telecommunication platforms in Koria," *EURASIP International Journal of Communications and Networking*, Vol. 2008, 596383, 2008, Doi: 1155/2008/596383.
5. Dessouky, M., H. Sharshar, and Y. Albagory, "Improving the cellular coverage from a high altitude platform by novel tapered beamforming technique," *Journal of Electromagnetic Waves and Applications*, Vol. 21, No. 13, 1721–1731, 2007.
6. Hofmann-Wellenhof, B., H. Lichtenegger, and J. Collins, *Global Positioning System Theory and Practice,* 2nd Edition, 1993, Print ISBN: 978-3-211-82477-1, Online ISBN: 978-3-7091-3293-7.
7. Krim, H. and M. Viberg, "Two decades of array signal processing research," *IEEE Signal Processing Magazine*, Vol. 13, No. 4, 67–94, Jul. 1996.
8. Harabi, F., A. Gharsallah, and S. Marcos, "Three-dimensional antennas array for the estimation of direction of arrival," *IET Microwaves, Antennas & Propagation*, Vol. 3, No. 5, 843–849, Aug. 2009.
9. Zhang, X., M. Zhou, H. Chen, and J. Li, "Two-dimensional DOA estimation for acoustic vector-sensor array using a successive MUSIC," *Multidimensional Systems and Signal Processing*, Vol. 25, No. 3, 583–600, Jul. 2014.
10. Agatonović, M., Z. Stanković, I. Milovanović, N. Dončov, L. Sit, T. Zwick, and B. Milovanović, "Efficient neural network approach for 2D DOA estimation based on antenna array measurements," *Progress In Electromagnetics Research*, Vol. 137, 741–758, 2013.
11. Diab, W. G. and H. M. Elkamchouchi, "A deterministic approach for 2D-DOA estimation based on a V-shaped array and a virtual array concept," *IEEE 19th International Symposium on Personal, Indoor and Mobile Radio Communications, PIMRC 2008*, 1–5, 2008.
12. Lee, J., I. Song, H. Kwona, and S. R. Lee, "Low-complexity estimation of 2D DOA for coherently distributed sources," *Signal Processing*, Vol. 83, No. 8, 1789–1802, Aug. 2003.
13. Schulz, D. and R. S. Thomae, "Search-based MUSIC techniques for 2D DOA estimation using EADF and real antenna arrays," *WSA 2013 — 17th International ITG Workshop on Smart Antennas*, 1–8, Stuttgart, Deutschland, 2013.
14. Raich, R., J. Goldberg, and H. Messer, "Bearing estimation for a distributed source via the conventional beamformer," *Ninth IEEE SP Workshop on Statistical Signal and Array Processing, Proceedings*, 5–8, Sep. 14–16, 1998.
15. Zhang, X., J. Li, and L. Xu, "Novel two-dimensional DOA estimation with L-shaped array," *EURASIP Journal on Advances in Signal Processing*, Vol. 2011, 50, Aug. 2011.